JPE 8-2-7

A Study on the PCS Characteristics of a 10kW BIPV System

Hyung-Sang Yoon†, In-Su Cha*, Jeong-Phil Yoon**, Jeong-Il Lee*** and Jang-Su Seo***

†*Dept. of Electrical and Electronics Eng., Dongshin University, Jeonnam, Korea
**Fusion Information Tech. Co. Ltd
***Dept. of Digital Electrical. Songwon College

ABSTRACT

A BIPV(Building Integrated PV) system is united by a constituent outer covering and can expect dual effects that reduce expenses for the establishment of a PV system. It is a profitable technology because it does not need a building as it is a stand alone PV system.

In this paper, output characteristics analysis of PCS and web-based monitoring of 10kW BIPV, were stimulated and examined for validity. The BIPV system proposed in this paper was established in at BIC (Biotechnology Industrialization Center) of Dongshin University, which was composed with PCS and Web-monitoring system.

Keywords: BIPV, PV system, Monitoring, PCS

1. Introduction

As buildings have become larger and equipped with more information and automation, demand for power has skyrocketed. Accordingly, mass research on generation equipment utilizing new types of energy is currently being conducted. As use of power has become greater, power outages would cause great tangible and intangible economic losses. Under these conditions, the demand for stable and reliable in generators has risen.

Generators utilizing new types of energy can only be dealt with by technicians, who have professional knowledge and required skills. Because of this, currently there are managers at generator sites, but these people are experiencing difficulties due to the lack of professional knowledge. The current safety management process is a temporary on-site equipment check. It is a minimal procedure and it is difficult to conduct every day. This process is very limited in forecasting future accidents, which makes it difficult to increase efficiency. New equipment has been developed to enable the user to monitor and control the generating facilities in remote locations, using computers and information communications equipment, which results in better stability and reliability.[1]-[3]

The current study will analyze the characteristics of PCS of 10kW BIPV through simulations and system monitoring.

Manuscript received Dec. 10, 2007; revised Feb. 18, 2008
† Corresponding Author: hl4rkb@naver.com
Tel: +82-61-330-2860, Fax: +82-61-330-2860, Dongshin Univ.
*Dept. of Hydrogen & Fuelcell Tech., Dongshin University
** Fusion Information Tech. Co. Ltd
*** Dept. of Digital Electrical. Songwon College

2. Discussion

To provide photovoltaic(PV) generated power to existing loads, the direct current power, acquired from the PV generation must be converted into AC power, which is

the same with commercial power. This kind of direct-AC conversion is carried out by an inverter, and the inverter is an essential part of PV generation. Also, the inverter balances power between the power source and load. An independent inverter provides all power, including valid and invalid power, as the load requires. The system connection inverter runs in conjunction with the system. When the inverter's output is a single square wave, harmonic contents are included in the output. Therefore, the harmonic contents must be removed from the square wave, and only the square wave must be put through output with a filter. When the impedance of the square wave filter is high, the output voltage changes greatly with rapid load current change. Therefore, it is advisable to have a small square wave filter. The PI controller has a simple design and can compose an adequate controller for this purpose. Relative controllers stabilize systems and reduce errors during normal conditions by magnifying errors. However, when the normal condition is set, over interest to reduce these errors cause overshoots. To reduce this kind of normal status error, integrating controllers are used, but this causes vibrations, which increase the range of the controller and might damage system stability.

Fig. 1 is a block diagram of the PI voltage controller. The output voltage is fed back and the difference with standard voltage is inputted into the PI controller. The dynamics of this controller is somewhat limited due to the delay of the control, and this is clearly evident when the load is not linear. To improve the dynamics caused by load change, the load current can be fed forward to compensate. This is a form of inserting the load current at the back part of the PI controller, and better results are shown when the calculated load value of a sample time is fed forward.

The PI current control process compares the triangular wave and standard signal, and is called the triangular wave comparison method. Fig. 2 shows a block diagram of the PI controller.

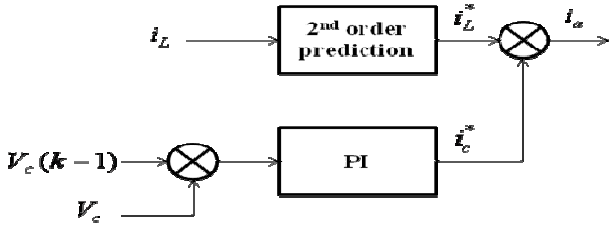

Fig. 1 Block diagram of PI Voltage controller

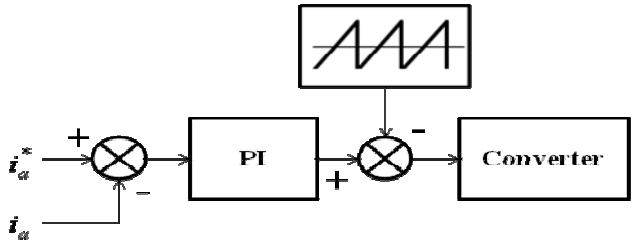

Fig. 2 Block diagram of PI Current controller

If the average voltage of the front end of the inverter L-C filter is V_a

$$V_a = K_S V_{cont} \tag{1}$$

In equation (1), V_{cont} is the output of the PI current controller, and K_s is the system gain.

Here the flowing current is:

$$i_a = \frac{V_a}{Z_{eq}} \tag{2}$$

In equation (2), Z_{eq} includes the inverter internal impedance, filters internal impedance, and load impedance. If the gain of the PI controller is G, the PI controller's output, V_{cont} is as follows.

$$G(i_a^* - i_a) = V_{cont} \tag{3}$$

From equation (3)

$$G(i_z^* - i_a) = \frac{V_a}{K_s} = \frac{1}{K_s} Z_{eq} \cdot i_a \tag{4}$$

$$i_a = \frac{G}{\frac{Z_{eq}}{K_s} + G} i_a^* \tag{5}$$

If $G = \frac{K_i + j\omega K_p}{j\omega}$, equation (6) is derived,

$$i_a = \frac{1}{\frac{Z_{eq}}{K_s}\frac{K_i + j\omega}{j\omega} + 1} i_a^* \tag{6}$$

In the above equation, if K_i is not infinite, the real current standard cannot be found, and errors can occur in normal status. Therefore, to compensate, K_i of the system must be as large as possible. The current study compares the PI voltage controller and the PI current controller through simulation and experiments, and the characteristics were compared and analyzed.

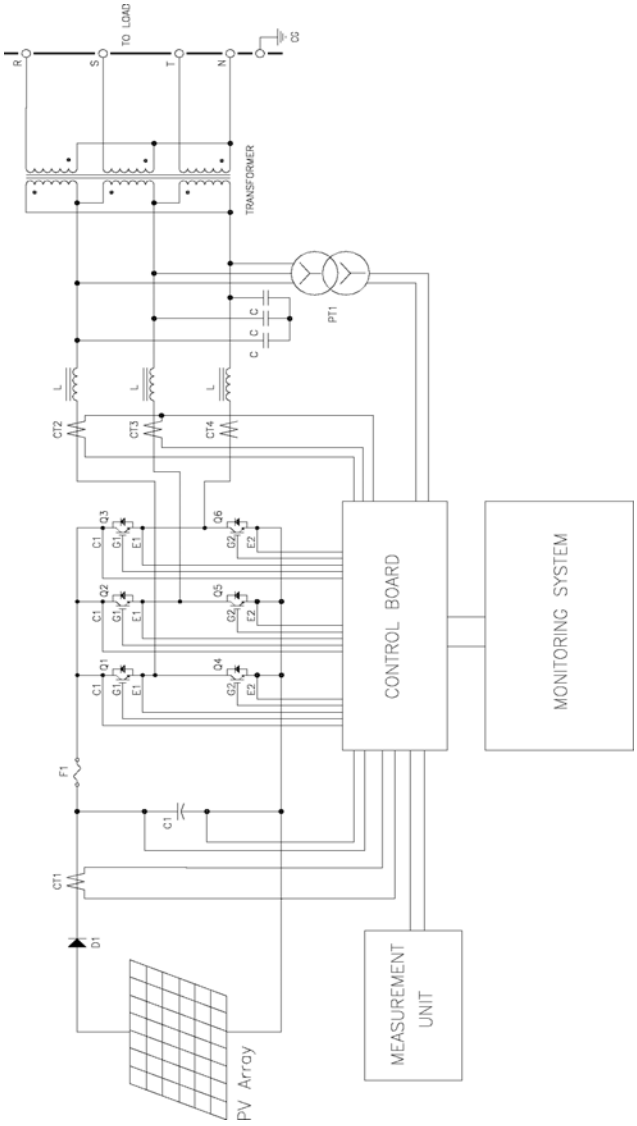

Fig. 3 Block diagram of BIPV System

Fig. 3 shows the BIPV system. It is composed of 3 10kW PCS, and a monitoring system was used to analyze the output characteristics.

The PV generator system is a system connection type, and the monitoring system has a sensor that senses voltage and current, and an add-on card, which sends information.

LABVIEW was used as the monitoring software. Since low harmonic contents were included in the output when the output of the inverter is a single square wave, a square wave filter is required to output only the standard square wave contents. When the impedance of the square wave filter is high, the output voltage changes greatly with rapid load current change.

Therefore, it is advisable to have a small square wave filter. The power variation range, in connection with normal operating generation output change and control variation, must be within 220V±10%. The power factor, within the range of 1/2 of the regular output and output, must be within ±0.95. This study considers the power quality, model and simulation of the 3 phase PCS. Table 1 shows the specifications of the PCS.

Table 1 Specification of PCS

Item	Specification
Input voltage	DC 252 ~ 400 [V]
Output voltage	AC 220 [V] ± 10%
Output power	10 [kVA] ± 10%
Output frequency	60 [Hz] ± 10%
Type	PWM, 3Φ
Security gadget	over voltage(350), low current(180)
Power factor	within 0.95
Max. efficiency	93.9 [%]

3. PCS Characteristics and Analysis

Fig. 4 shows the circuit and control block diagram of the 10kW 3 phase PCS. The power circuit is composed of the reactor, DC link condenser, and the IGBT, a power device. The PCS is also composed of the power voltage detector, which synchronizes the phase, the voltage controller that controls the voltage of the DC link, current controller, 2 phase – 3 phase and stop-rotate coordinate converter, and the gate driving circuit, which drives the power devices in PWM.

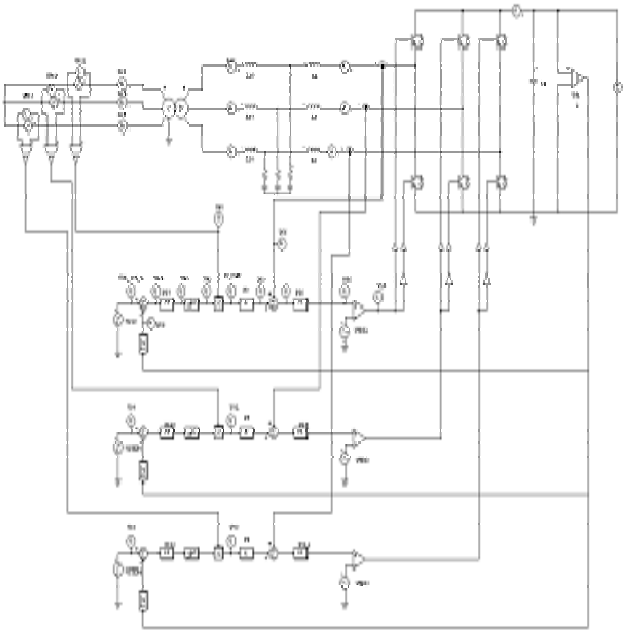

Fig. 4 Simulation circuit of PCS

The IGBT prevents over voltage shocks, and is composed of a snubber resistance and snubber capacitor to prevent over currents during turn-on. By using the freewheeling diode, switching is made easier for the load inductance current energy circulation.

With the 3 phase converter, the zero point of the power voltage on u, v, w is analyzed to see whether the 3 phase is in normal or reverse order for the rotation direction. Also, the rotation angle speed and rotation angle are set so that the power voltage vector from the w phase zero point coincides with the q axis on the rotation coordinate.

Only the sensor output of the u and v phases are A/D converted, and the w phase is calculated assuming the 3 phase parallel.

This 3 phase current is converted through 3 phase-2phase and stationary coordinates-rotation coordinates and is express in d and q in the rotation coordinate. Values of d and q are controlled with the PI controller, and the d and q voltage order is converted through rotation coordinates-stationary coordinates and 2 phase-3 phase.

PWM signals, which use triangular wave comparison, are made, and the IGBT is driven through the gate driving circuit. Here the gate carrier signal is a triangular wave of 10 kHz, and the reference signal is a square wave of 60Hz.

Fig. 5 shows the inverter switching signal, output voltage, and output current under constant load, Out of the PCS's output, only the u phase is a wave that is magnified during one cycle, which shows that output voltage and current are normal.

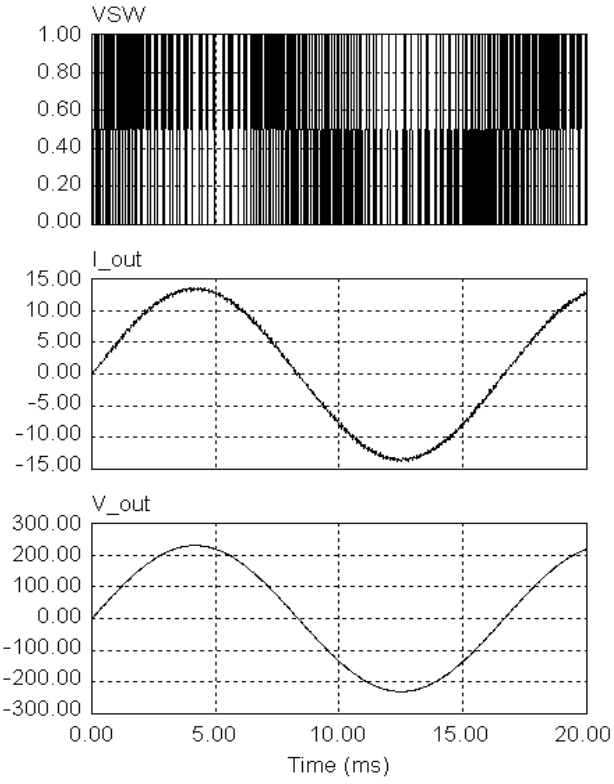

VSW : Switching signal
V_out : Output voltage
I_out : Output current

Fig. 5 Switching signal, output voltage and current of PCS

Fig. 6 shows the output voltage and current of the PCS's u, v, and w phase in normal status. The output voltage and current is output with 120。 phase difference.

Fig. 7 shows the PCS's voltage-current output and FFT characteristics through voltage control. Although the voltage controller is good, some ±2V discrepancy is shown in the current characteristics. Also the switching movement is not stable.

Fig. 8 shows the PCS's voltage-current output and FFT characteristics through current control. Although there is great discrepancy in voltage control, the voltage-current

output is stable, and the discrepancy rate dropped to ±1 V. The switching movement is also stable. The PCS becomes more stable when more current is applied to the current controller than to the voltage controller.

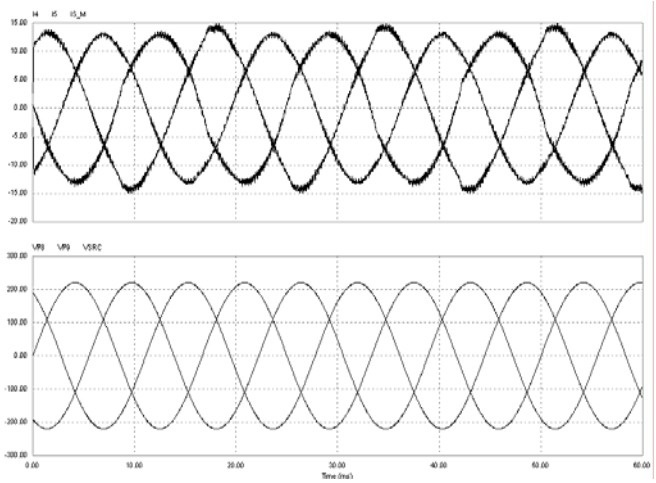

Fig. 6 Phase voltage and current of PCS

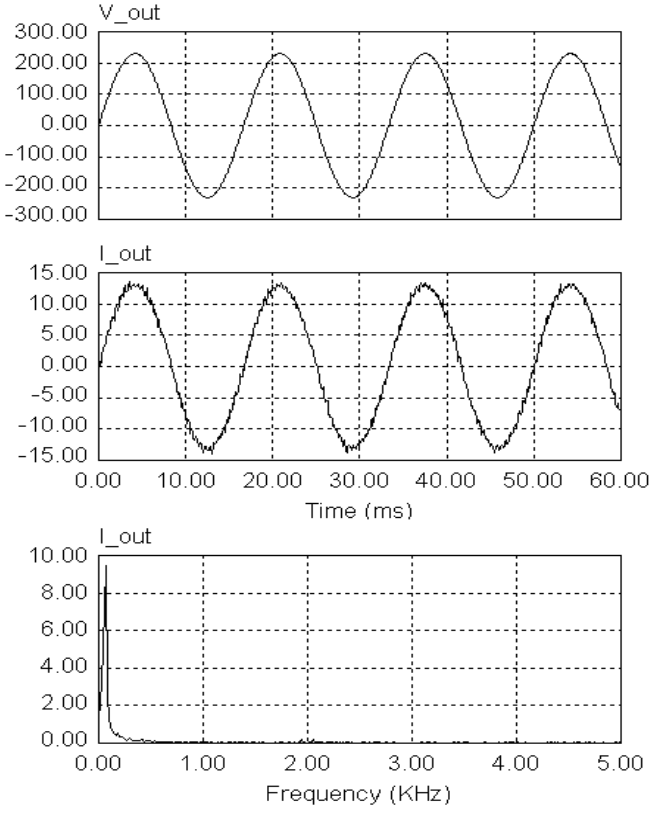

Fig. 7 PCS output characteristic of PI voltage controller

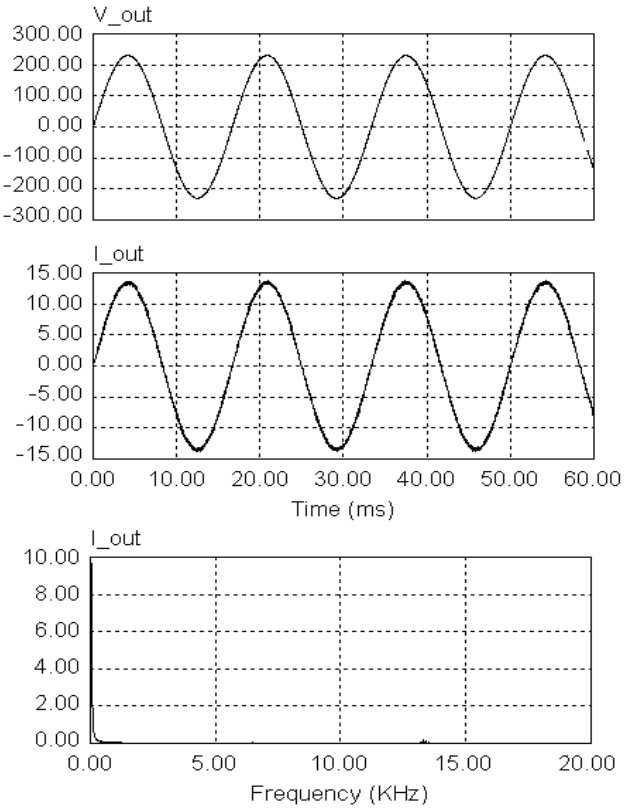

Fig. 8 PCS output characteristic of PI current controller

4. Characteristics Analysis through Monitoring

Fig. 9 and 10 show the voltage-current-power characteristics of the PCS output with solar radiation under PI current control and voltage control. When solar radiation increases, output power also increases. When the PI current controller is applied, the voltage change is somewhat large when the solar radiation is below 200W/㎡.

However, when the solar radiation is over 200W/㎡, the variation range is 224[V] ~ 229[V], which is within the standard of 220[V]±10%. The distribution of points is close to a line, which shows that the quality of output is high. When solar radiation is 800.2[W/㎡], 3522[W] is produced. However, only 2910[W] is produced at 802.63[W/㎡], which shows that the output is not stable. In conclusion, the PI current controller has better power quality than that of the PI voltage controller.

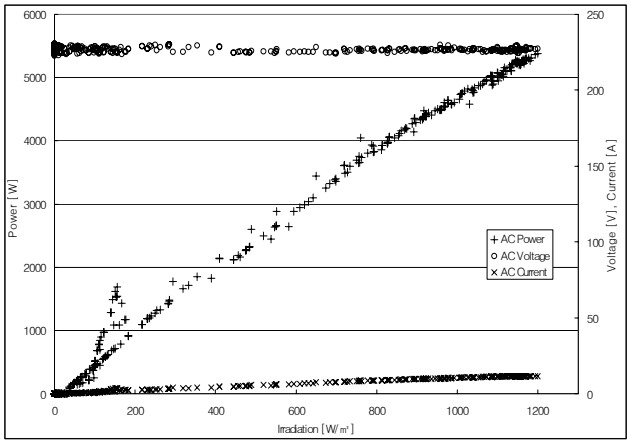

Fig. 9 Output voltages and current, power characteristic of PCS for BIPV according to irradiation variation (PI current control)

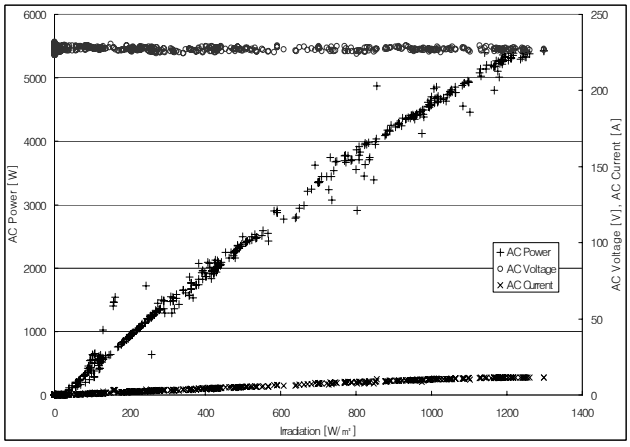

Fig. 10 Output voltages and current, power characteristic of PCS for BIPV according to irradiation variation (PI voltage control)

Fig. 11 shows the power, voltage, and current characteristics of the BIPV array according to changes in the environment, such as solar radiation and temperature. When solar radiation increases, so does the output power. The power is at a maximum at 8970[W] when the solar radiation is the highest at around 1300 hours. Also, the characteristic curve shows that the weather is clear.

Under standard conditions(1000W/㎡, 25℃), the output of the solar radiation array is calculated as 10,440[W], and the actual output is 8970[W]. The arrays output efficiency is at 87%. This shows that the lining installation of the PV array is stable. Fig. 12 shows the voltage, current, and output characteristics of the PCS. At around 1300 hours, the current is at its maximum at 11.9[A], which shows that the solar radiation is at maximum. Although there are variations in voltage and current from these figures, it runs regularly.

Fig. 13 shows the voltage, current, and output characteristics of the BIPV array, according to temperature change. Although there might be measuring errors in temperature, the array's surface temperature moves between 12℃ and 28℃. As the temperature rises, the output voltage, current, and power of the array increases, and gains maximum output at 25℃. Therefore, in order to calculate the array's output power with surface temperature change, the measuring location and method must be reviewed.

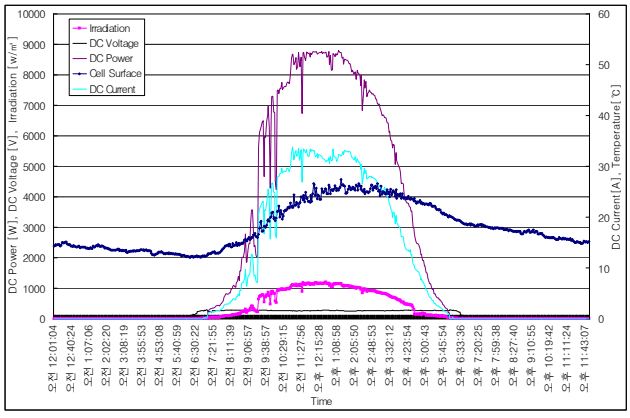

Fig. 11 Output characteristic of BIPV array

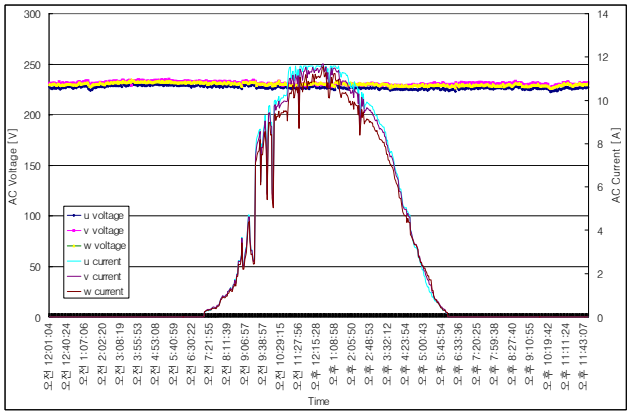

Fig. 12 Output voltages and current character istic of PCS

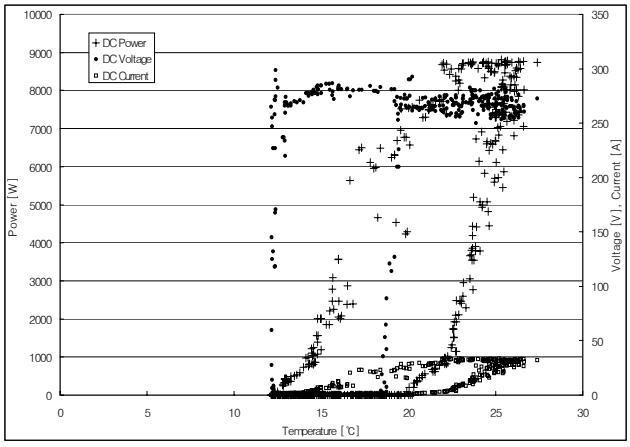

Fig. 13 Output voltage and current, power characteristic of BIPV array according to temperature

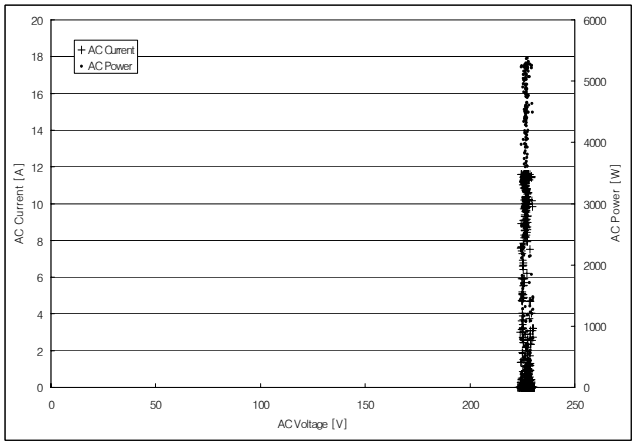

Fig. 15 Output V-I and V-P characteristic of PCS

Fig. 14 shows the voltage-current, voltage-power characteristics of the DC link. The output voltage range is 250[V] ~ 290[V] and the maximum current is 33[A], while the maximum power is 8970[W]. Also the maximum power is found when voltage is 260[V] ~ 280[V] and current is 31[A] ~ 33[A]. Figure 15 shows the voltage-current characteristics of the PCS. The voltage range is AC 222[V] ~ 228[V], and the maximum current is 11.9[A]. At maximum power, voltage is 225[V] ~ 226[V], current is 11.9[A], and power is 5,500[W]. From these figures, we can see that the inverter operation follows the maximum output point and is improving the generation capability.

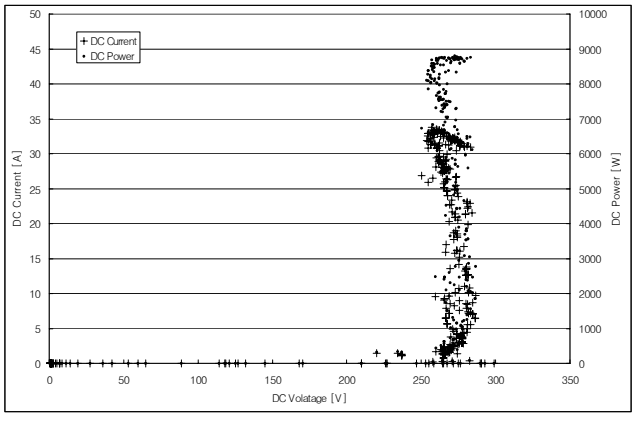

Fig. 14 Output current and power characteristic of DC link according to voltage

5. Conclusions

This paper, through simulation of a 10kW BIPV PCS, analyzed the system and applied findings to the actual system. Web-based remote monitoring was conducted to make a database of the characteristics of the actual system. First, the BIPV system's PCS output characteristics were analyzed through simulation, and were proven through experimentation. To supplement the discontinuous generating characteristic of the PV generator, an inverter was used. The PI voltage control method and PI current control method, applied in simulation with the PCS, were compared. As the control method for the BIPV PCS, PI voltage control and PI current control were proposed, and the characteristics were analyzed through simulation and experimentation. PI current control had voltage ranges of 224[V] ～ 229[V], which were operating within the standard condition of 220[V]±10%. The distribution of power was close to a line, which shows that the quality of power is high. When the PIC voltage controller was applied, the voltage range was 224[V]～229[V] when solar radiation increased, which met the standard condition of 220[V]±10%. However, the distribution of power was much greater than the PI current controller. For example, the output at 800.2[W/㎡] was 3522[W], while it was 2910[W] at similar conditions of 802.63[W/㎡].

Also, after analyzing the PCS's square wave characteristic through FFT, the PI current controller had 2% distortion, while the PI voltage controller had 4.5%.

The distortion in real life was greater than that of the simulation. This can be improved when the simulation is converted into a program. All system components were analyzed remotely through a monitoring system, and the system output levels were analyzed according to changes in the environment. The maximum difference between the real data and data in theory was only 0.4%, which was a good result. When the BIPV system was applied to a building with similar conditions, good data resulted. When the system connecting the inverter's output was reduced and disconnected with the system line, residual power was developed. This needs to be improved. Although there are many ways to solve the residual power problem, it would be adequate to provide emergency lights, which would be used during blackouts. Batteries and safety devices would be needed for the use of emergency lights.

Acknowledgment

This work was supported by a grant from KEPRI and KESRI R-20050B117

References

[1] G. L. Campen, "An Analysis of the Harmonics and Power Factor Effects at a Utility Intertied Photovoltaic System", IEEE Trans. Vol. PAS-101, No. 12, pp. 4632-4639, 1982.

[2] Yourstone, S.A. "Realtime Process Quality Control in Computer Integrated Manufacturing", marcel Dekker, 1991.

[3] Gwonjong Yu, Jinsoo Song, "Development of Power Converter for Photovoltaic System", Japan-Korea Joint Seminar on TECHNICAL DIGEST PHOTOVOLTAICS, pp. 247-254, 1995.

Hyung-Sang Yoon was born in Bosung County, Jeonnam Prefecture, Korea, in 1969. He received the B.S. degree in Dept. of Electronics Eng. Dongshin Univ., in 1992. Also, he respectively received the M.S. and Ph.D. degrees in Dept. of Electrical & Electronics Eng. Dongshin Univ., Naju, Jeonnam, Korea, in 1998 and 2008. Currently, he is a CEO, Fusion Information Tech. Co. Ltd.. He is a member of KIPE, KIEE.

In-Su Cha was born in Yeosu, Jeonnam Prefecture, Korea, in 1959. he received the B.S. degree in Dept. of Electrical Eng., Chosun Univ., in 1982. Then, he received the M.S. degree in Dept. of Electrical Eng., Chung-Ang Univ., in 1984. Respectively, he received the Ph.D. degree in Dept. of Electrical Eng. Chosun Univ., Gwangju, Korea, in 1989. Currently, he is a professor at Dept. of Hydrogen & Fuelcell Tech., Dongshin Univ., Naju, Jeonnam, Korea. He is a member of IEEE, KIPE, KIEE.

Jeong-Phil Yoon was born in Gwangju, Korea, in 1977. He received the B.S. degree in Dept. of Electronics Eng. Dongshin Univ., in 2001. He respectively received the M.S. and Ph.D degrees in Dept. of Electrical & Electronics Eng. Dongshin Univ., Naju, Jeonnam Prefecture, in 2003 and 2007. Currently, he is a Senior researcher at Fusion Information Tech. Co. Ltd.. He is a member of KIPE, KIEE.

Jeong-Il Lee was born in Gwangju, Korea, in 1967. He received the B.S. degree in Dept. of Electrical Eng. Gwangju Univ., in 1996. Then, he received the M.S. degree in Dept. of Electrical Eng. Chosun Univ., in 1999. Respectively, he received the Ph.D. degree in Dept. of Electrical & Electronics Eng. Dongshin Univ., Naju, Jeonnam Prefecture, Korea, in 2003. Currently, he is a Professor at Dept. of Digital Electrical, Songwon Community College in Gwangju, Korea. He is a member of KIPE, KIEE.

Jang-Soo Seo was born in Yeochun County, Jeonnam Prefecture, Korea, in 1951. He received the B.S. degree in Dept. of Electrical Eng. Chosun Univ., in 1982. Then, he respectively received the M.S. and Ph.D. degrees in Dept. of Electrical Eng. Chosun Univ., Gwangju, Korea, in 1985. Currently, he is a Professor at Dept. of Digital Electrical, Songwon Community College in Gwangju, Korea. He is a member of KIPE, KIEE.